

# Spin density matrix for neutral $\rho$ mesons in a pion gas in linear response theory

Yi-Liang Yin,<sup>1</sup> Wen-Bo Dong,<sup>1</sup> Cong Yi,<sup>1</sup> and Qun Wang<sup>1,2</sup>

<sup>1</sup>*Department of Modern Physics and Anhui Center for Fundamental Sciences in Theoretical Physics,  
University of Science and Technology of China, Hefei, Anhui 230026, China*

<sup>2</sup>*School of Mechanics and Physics, Anhui University of Science and Technology, Huainan, Anhui 232001, China*

We calculate the spin density matrix for neutral  $\rho$  mesons from the spectral function and thermal shear tensor by Kubo formula in the linear response theory, which contributes to the  $\gamma$  correlator for the CME search. We derive the spectral function of neutral  $\rho$  mesons with  $\rho\pi\pi$  and  $\rho\rho\pi\pi$  interactions using the Dyson-Schwinger equation. The thermal shear tensor contribution is obtained from the Kubo formula in the linear response theory. We numerically calculate  $\rho_{00} - 1/3$  and  $\text{Re}\rho_{-1,1}$  using the simulation results for the thermal shear tensor by the hydrodynamical model, which are of the order  $10^{-3} \sim 10^{-2}$ .

## I. INTRODUCTION

The spin and orbital angular momentum are intrinsically connected and can be converted to each other as demonstrated in the Barnett effect [1] and Einstein-de-Haas effect [2] in materials. In non-central heavy-ion collisions, a huge orbital angular momentum is generated and partially transferred to the strongly interacting matter in the form of particle's spin polarization along the reaction plane through spin-orbit couplings [3]. This phenomenon is called the global spin polarization as it is with respect to the reaction plane which is fixed for all particles in one event [3–8]. The global spin polarization of  $\Lambda$  and  $\bar{\Lambda}$  hyperons was first observed and measured in the STAR experiment [9, 10], and then measured in experiments of HADES [11] and ALICE [12]. Since its first observation [9, 10], there has been tremendous advance in the study of the global spin polarization in theoretical models [13–23], see Refs. [24–32] for recent reviews on this topic.

The spin polarization of hyperons can be measured through their parity-breaking weak decays [33]. Vector mesons mostly decay through parity-conserved strong interaction, so there is no way to measure the spin polarization of vector mesons. The spin states of the vector meson can be described by the spin density matrix  $\rho_{\lambda_1\lambda_2}$ , where  $\lambda_1$  and  $\lambda_2 = 0, \pm 1$  denote the spin states. The spin density matrix is normalized  $\text{tr}\rho \equiv \sum_{\lambda} \rho_{\lambda\lambda} = 1$ . The  $\rho_{00}$  element can be measured in experiments through the polar angle distribution of decay products [5, 34–36]. If  $\rho_{00} \neq 1/3$ , the spin-0 state of the vector meson is not equally populated as  $\lambda = \pm 1$  states, which is called the spin alignment. Specifically,  $\rho_{00} < 1/3$  means the field vector (not the spin vector) is more aligned to the direction perpendicular to the spin quantization direction, while  $\rho_{00} > 1/3$  means the field vector is more aligned to the spin quantization direction. The spin alignment with respect to the reaction plane is called the global spin alignment and was also predicted in 2004-2005 [5]. The global spin alignment of  $\phi$  and  $K^{0*}$  mesons has recently been measured by the STAR collaboration in Au+Au collisions [37], where a large deviation of  $\rho_{00}$  for  $\phi$  mesons from 1/3 is observed at lower collision energies, but there is no significant deviation of  $\rho_{00}$  for  $K^{0*}$  mesons within errors.

A number of sources can contribute to the spin alignment of  $\phi$  mesons but not enough to explain such a large effect [35, 38–41]. It was proposed that a large spin alignment of  $\phi$  mesons may come from the local correlation/fluctuation of strong vector fields that are coupled to s and  $\bar{s}$  quarks [42]. Initially a nonrelativistic quark coalescence model [35] was used to calculate the spin density matrix of  $\phi$  mesons with s and  $\bar{s}$  quarks being polarized by strong vector fields [43]. Then the nonrelativistic quark coalescence model was generalized to a relativistic one [44, 45]. The relativistic model is based on Wigner functions and spin kinetic equations for vector mesons. The model incorporated with strong vector fields can successfully describe the experimental data for the global spin alignment of  $\phi$  mesons [44–46]. For recent reviews of the topic, the readers may look at Refs. [47–50].

Recently, the thermal shear contribution to  $\phi$  meson's spin alignment has been studied in the linear response theory [51, 52]. In this paper, we will apply the same method to another vector meson, the neutral rho meson or  $\rho^0$ . The spin density matrix of  $\rho^0$  may serve as a background for the chiral magnetic effect (CME) [53–55], because the anisotropic angular distribution of its decay daughters (pions) provides a non-vanishing contribution to the  $\gamma$  correlator [56–59], see Refs. [60, 61] for quantitative analyses. In Ref. [62] by some of us, the evolution of  $\rho^0$  mesons in a pion gas was studied by the spin kinetic or Boltzmann equation for the on-shell spin dependent distribution. The results show that the spin alignment of  $\rho^0$  mesons is damped rapidly in the pion gas due to  $\rho\pi\pi$  interaction and that  $\rho_{00}$  and  $\text{Re}\rho_{-1,1}$  have a significant contribution to the  $\gamma$  correlator for CME. In this paper, we will consider the off-shell contribution as well as the thermal shear contribution to  $\rho_{00}$  and  $\text{Re}\rho_{-1,1}$  by assuming thermal spin distributions for  $\rho^0$ . We will treat the thermal shear tensor as a perturbation from local equilibrium and apply the Kubo formula [63–65] to calculate the linear response of the spin density matrix for  $\rho^0$  mesons as done for  $\phi$  mesons in Refs. [51, 52]. The spectral function of  $\rho^0$  mesons is derived from  $\rho\pi\pi$  and  $\rho\rho\pi\pi$  interaction in the chiral effective theory [66]. Finally, we present numerical results for  $\rho_{00}$  and  $\text{Re}\rho_{-1,1}$  of  $\rho^0$  mesons using the simulation results for the thermal shear tensor from the hydrodynamical model [23, 67, 68].

The paper is organized as follows. In Sec. II, we briefly introduce the Green's functions for vector mesons and pseudoscalar mesons in closed-time-path (CTP) formalism. In Sec. (III), we define the Wigner function and the matrix valued spin dependent distribution (MVSD) for the  $\rho^0$  meson which is proportional to its spin density matrix. In Sec. (IV), we use the Dyson-Schwinger equation to derive the spectral function of the  $\rho^0$  meson. We also derive the explicit form of the Wigner function without nonlocal terms. In Sec. (V), we obtain the nonlocal correction to the Wigner function proportional to the thermal shear tensor through the Kubo formula in the linear response theory. The numerical results are presented in Sec. (VI) and a summary of results and the conclusion are given in the last section.

By convention, the metric tensor is  $g^{\mu\nu} = \text{diag}(1, -1, -1, -1)$ , four-momenta are denoted as  $p^\mu = (p_0, \mathbf{p})$ ,  $p_\mu = (p_0, -\mathbf{p})$ , where  $\mu, \nu = 0, 1, 2, 3$ , and Greek letters and Latin letters represent space-time components of four-vectors and space components of three-vectors respectively. For notational clarification, we use  $G^{\mu\nu}$  and  $p$  for the two-point Green's function and momentum for the  $\rho^0$  meson, while  $S$  and  $k$  for the two-point Green's function and momentum for the pseudoscalar meson  $\pi^\pm$ .

## II. GREEN'S FUNCTION IN CLOSED-TIME-PATH FORMALISM

The closed-time-path (CTP) or Schwinger-Keldysh formalism in quantum field theory is an effective method to describe equilibrium and non-equilibrium physics in many-body systems [69–76]. The two-point Green's functions on the CTP for the spin-1 vector meson ( $\rho^0$ ) and spin-0 pseudoscalar meson ( $\pi^\pm$ ) are defined as

$$\begin{aligned} G_{\text{CTP}}^{\mu\nu}(x_1, x_2) &= \langle T_C A^\mu(x_1) A^\nu(x_2) \rangle, \\ S_{\text{CTP}}(x_1, x_2) &= \langle T_C \phi(x_1) \phi^\dagger(x_2) \rangle, \end{aligned} \quad (1)$$

where  $T_C$  denotes the time-ordered operator on the CTP, and  $A^\mu$  and  $\phi$  are the real vector field and complex scalar field respectively, which can be quantized as

$$\begin{aligned} A^\mu(x) &= \sum_{\lambda=0, \pm 1} \int \frac{d^3 p}{(2\pi)^3} \frac{1}{2E_p^\rho} \\ &\quad \times \left[ \epsilon^\mu(\lambda, \mathbf{p}) a_V(\lambda, \mathbf{p}) e^{-ip \cdot x} + \epsilon^{\mu*}(\lambda, \mathbf{p}) a_V^\dagger(\lambda, \mathbf{p}) e^{ip \cdot x} \right], \\ \phi(x) &= \int \frac{d^3 k}{(2\pi)^3} \frac{1}{2E_k^\pi} \left[ a(\mathbf{k}) e^{-ik \cdot x} + b^\dagger(\mathbf{k}) e^{ik \cdot x} \right], \end{aligned} \quad (2)$$

where  $p = (E_p^\rho, \mathbf{p})$  and  $k = (E_k^\pi, \mathbf{k})$  are on-shell momenta for  $\rho$  and  $\pi$  with  $E_p^\rho = \sqrt{\mathbf{p}^2 + m_\rho^2}$  and  $E_k^\pi = \sqrt{\mathbf{k}^2 + m_\pi^2}$ ,  $\lambda$  denotes the spin state, and  $\epsilon^\mu(\lambda, \mathbf{p})$  is the spin polarization vector

$$\epsilon^\mu(\lambda, \mathbf{p}) = \left( \frac{\mathbf{p} \cdot \boldsymbol{\epsilon}_\lambda}{m_\rho}, \boldsymbol{\epsilon}_\lambda + \frac{\mathbf{p} \cdot \boldsymbol{\epsilon}_\lambda}{m_\rho(E_p^\rho + m_\rho)} \mathbf{p} \right), \quad (3)$$

where  $\boldsymbol{\epsilon}_\lambda$  is the spin polarization three-vector in the particle's rest frame given by

$$\begin{aligned} \boldsymbol{\epsilon}_0 &= (0, 1, 0), \\ \boldsymbol{\epsilon}_{+1} &= -\frac{1}{\sqrt{2}}(i, 0, 1), \\ \boldsymbol{\epsilon}_{-1} &= \frac{1}{\sqrt{2}}(-i, 0, 1). \end{aligned} \quad (4)$$

We have chosen  $+y$  to be the spin quantization direction. The polarization vector satisfies

$$\begin{aligned} p_\mu \epsilon^\mu(\lambda, \mathbf{p}) &= 0, \\ \epsilon(\lambda, \mathbf{p}) \cdot \epsilon^*(\lambda', \mathbf{p}) &= -\delta_{\lambda\lambda'}, \\ -\sum_\lambda \epsilon^\mu(\lambda, \mathbf{p}) \epsilon^{\nu*}(\lambda, \mathbf{p}) &= \Delta^{\mu\nu}(p_{\text{on}}) \equiv g^{\mu\nu} - \frac{p^\mu p^\nu}{m_\rho^2}. \end{aligned} \quad (5)$$

Note that in the above equation,  $p^\mu$  is an on-shell momentum, so we put the index ‘‘on’’ to the momentum variable in the projector  $\Delta^{\mu\nu}(p_{\text{on}})$  to distinguish it from the off-shell projector  $\Delta^{\mu\nu}(p)$  which will be used later. We see in Eq. (2) that we use  $G$  and  $p$  to denote the Green's function and momentum for  $\rho^0$  respectively, while we use  $S$  and  $k$  to denote the Green's function and momentum for  $\pi^\pm$  respectively.

In the CTP formalism,  $G_{\text{CTP}}^{\mu\nu}$  in Eq. (1) has four components

$$\begin{aligned} G_F^{\mu\nu}(x_1, x_2) &\equiv \theta(t_1 - t_2) \langle A^\mu(x_1) A^\nu(x_2) \rangle + \theta(t_2 - t_1) \langle A^\nu(x_2) A^\mu(x_1) \rangle, \\ G_{<}^{\mu\nu}(x_1, x_2) &\equiv \langle A^\nu(x_2) A^\mu(x_1) \rangle, \\ G_{>}^{\mu\nu}(x_1, x_2) &\equiv \langle A^\mu(x_1) A^\nu(x_2) \rangle, \\ G_{\bar{F}}^{\mu\nu}(x_1, x_2) &\equiv \theta(t_2 - t_1) \langle A^\mu(x_1) A^\nu(x_2) \rangle + \theta(t_1 - t_2) \langle A^\nu(x_2) A^\mu(x_1) \rangle, \end{aligned} \quad (6)$$

depending on whether  $x_1$  and  $x_2$  are on the positive or negative time branch. One can verify that all four components satisfy the identity  $G_F^{\mu\nu} + G_{\bar{F}}^{\mu\nu} = G_{<}^{\mu\nu} + G_{>}^{\mu\nu}$ , so only three of them are independent which one can choose the retarded,

advanced and correlation Green's functions  $G_R^{\mu\nu}$ ,  $G_A^{\mu\nu}$  and  $G_C^{\mu\nu}$  as

$$\begin{aligned}
G_R^{\mu\nu}(x_1, x_2) &\equiv \theta(t_1 - t_2) (\langle A^\mu(x_1)A^\nu(x_2) \rangle - \langle A^\nu(x_2)A^\mu(x_1) \rangle) \\
&= G_F^{\mu\nu}(x_1, x_2) - G_{<}^{\mu\nu}(x_1, x_2), \\
G_A^{\mu\nu}(x_1, x_2) &\equiv \theta(t_2 - t_1) (\langle A^\nu(x_2)A^\mu(x_1) \rangle - \langle A^\mu(x_1)A^\nu(x_2) \rangle) \\
&= G_F^{\mu\nu}(x_1, x_2) - G_{>}^{\mu\nu}(x_1, x_2), \\
G_C^{\mu\nu}(x_1, x_2) &\equiv \langle A^\mu(x_1)A^\nu(x_2) \rangle + \langle A^\nu(x_2)A^\mu(x_1) \rangle \\
&= G_{<}^{\mu\nu}(x_1, x_2) + G_{>}^{\mu\nu}(x_1, x_2).
\end{aligned} \tag{7}$$

The four components of the Green's function for the complex scalar field can be defined similarly. Other operators can also be defined on the CTP, obeying the relations similar to Eq. (7) as

$$\begin{aligned}
O_R(x_1, x_2) &= O_F(x_1, x_2) - O_{<}(x_1, x_2), \\
O_A(x_1, x_2) &= O_F(x_1, x_2) - O_{>}(x_1, x_2), \\
O_C(x_1, x_2) &= O_{<}(x_1, x_2) + O_{>}(x_1, x_2),
\end{aligned} \tag{8}$$

where  $O$  is any operator defined on the CTP.

### III. WIGNER FUNCTIONS AND SPIN DENSITY MATRIX

In order to define the matrix valued spin dependent distribution (MVSD) for the vector meson in phase space, we introduce the Wigner transformation for the two-point Green's function that defines the Wigner function

$$G_{<}^{\mu\nu}(x, p) = \int d^4y e^{ip \cdot y} G_{<}^{\mu\nu} \left( x + \frac{1}{2}y, x - \frac{1}{2}y \right). \tag{9}$$

For free particles, the Wigner function has the form

$$\begin{aligned}
G_{(0)<}^{\mu\nu}(x, p) &= 2\pi \sum_{\lambda_1, \lambda_2} \delta(p^2 - m_V^2) \left\{ \theta(p^0) \epsilon^\mu(\lambda_1, \mathbf{p}) \epsilon^{\nu*}(\lambda_2, \mathbf{p}) f_{\lambda_1 \lambda_2}^{(0)}(x, \mathbf{p}) \right. \\
&\quad \left. + \theta(-p^0) \epsilon^{\mu*}(\lambda_1, -\mathbf{p}) \epsilon^\nu(\lambda_2, -\mathbf{p}) \left[ \delta_{\lambda_2 \lambda_1} + f_{\lambda_2 \lambda_1}^{(0)}(x, -\mathbf{p}) \right] \right\},
\end{aligned} \tag{10}$$

where the index “(0)” denotes the leading order of  $\hbar$ , and  $f_{\lambda_1 \lambda_2}^{(0)}(x, \mathbf{p})$  is the MVSD at leading order defined as

$$f_{\lambda_1 \lambda_2}^{(0)}(x, \mathbf{p}) \equiv \int \frac{d^4u}{2(2\pi)^3} \delta(p \cdot u) e^{-iu \cdot x} \left\langle a_V^\dagger \left( \lambda_2, \mathbf{p} - \frac{\mathbf{u}}{2} \right) a_V \left( \lambda_1, \mathbf{p} + \frac{\mathbf{u}}{2} \right) \right\rangle, \tag{11}$$

which satisfies  $f_{\lambda_1 \lambda_2}^{(0)*}(x, \mathbf{p}) = f_{\lambda_2 \lambda_1}^{(0)}(x, \mathbf{p})$ . Note that the MVSD can be decomposed into the scalar (trace), polarization ( $P_i$ ) and tensor ( $T_{ij}$ ) parts as [32, 48]

$$f_{\lambda_1 \lambda_2}^{(0)}(x, \mathbf{p}) = \text{Tr}(f^{(0)}) \left( \frac{1}{3} + \frac{1}{2} P_i \Sigma_i + T_{ij} \Sigma_{ij} \right)_{\lambda_1 \lambda_2}, \tag{12}$$

where  $i, j = 1, 2, 3$ ,  $\text{Tr}(f^{(0)}) = \sum_\lambda f_{\lambda\lambda}^{(0)}$ , and  $\Sigma_i$  and  $\Sigma_{ij}$  are traceless matrices defined in Eq. (11) of Ref. [77]. The on-shell part of the Wigner function  $W^{\mu\nu}(x, \mathbf{p})$  can be obtained by integration of  $(p_0/\pi)G_{(0)<}^{\mu\nu}(x, p)$  over  $p_0 = [0, \infty)$ . Using the decomposition (12)  $W^{\mu\nu}(x, \mathbf{p})$  can be decomposed into the scalar ( $\mathcal{S}$ ), polarization ( $G^{[\mu\nu]}$ ) and tensor ( $\mathcal{T}^{\mu\nu}$ ) parts as

$$W^{\mu\nu}(x, \mathbf{p}) = -\frac{1}{3} \Delta^{\mu\nu}(p_{\text{on}}) \mathcal{S} + G^{[\mu\nu]} + \mathcal{T}^{\mu\nu}, \tag{13}$$

where  $\mathcal{S}$ ,  $G^{[\mu\nu]}$  and  $\mathcal{T}^{\mu\nu}$  are defined in Eqs. (14) and (15) of Ref. [77].

According to Eq. (10), the MVSD can be inversely obtained from the Green's function as

$$\begin{aligned}
f_{\lambda_1 \lambda_2}^{(0)}(x, \mathbf{p}) &= \frac{1}{\pi} \int_0^\infty dp_0 p_0 \epsilon_\mu^*(\lambda_1, \mathbf{p}) \epsilon_\nu(\lambda_2, \mathbf{p}) G_{(0)<}^{\mu\nu}(x, \mathbf{p}), \\
\text{Tr} f^{(0)}(x, \mathbf{p}) &= -\frac{1}{\pi} \int_0^\infty dp_0 p_0 \Delta_{\mu\nu}(p_{\text{on}}) G_{(0)<}^{\mu\nu}(x, \mathbf{p}).
\end{aligned} \tag{14}$$

We assume that above relations hold at any order

$$\begin{aligned} f_{\lambda_1\lambda_2}(x, \mathbf{p}) &= \frac{1}{\pi} \int_0^\infty dp_0 p_0 \epsilon_\mu^*(\lambda_1, p) \epsilon_\nu(\lambda_2, p) G_{<}^{\mu\nu}(x, p), \\ \text{Tr}f(x, \mathbf{p}) &= -\frac{1}{\pi} \int_0^\infty dp_0 p_0 \Delta_{\mu\nu}(p) G_{<}^{\mu\nu}(x, p), \end{aligned} \quad (15)$$

where we have generalized the polarization (field) vector  $\epsilon^\mu(\lambda, \mathbf{p})$  to the off-shell four-momentum  $p$

$$\epsilon^\mu(\lambda, p) \equiv \left( \frac{\mathbf{p} \cdot \epsilon_\lambda}{\sqrt{p^2}}, \epsilon_\lambda + \frac{\mathbf{p} \cdot \epsilon_\lambda}{\sqrt{p^2}(p^0 + \sqrt{p^2})} \mathbf{p} \right). \quad (16)$$

One can check that  $\epsilon^\mu(\lambda, p)$  satisfies

$$-\sum_\lambda \epsilon^\mu(\lambda, p) \epsilon^{\nu*}(\lambda, p) = \Delta^{\mu\nu}(p) \equiv g^{\mu\nu} - \frac{p^\mu p^\nu}{p^2}. \quad (17)$$

In this paper we use the off-shell field vector, which is different from our previous work in Ref. [52], because the off-shell effect for the  $\rho^0$  meson is much more significant than the  $\phi$  meson and the expansion in powers of  $(p^0 - E_p)$  for  $\rho^0$  does not work well.

In order to calculate the spin density matrix  $\rho_{\lambda_1\lambda_2}$  which is the normalized  $f_{\lambda_1\lambda_2}$ ,  $\rho_{\lambda_1\lambda_2} \equiv f_{\lambda_1\lambda_2}/\text{Tr}f$ , from the Wigner function, we define the projector

$$L_{\mu\nu}(\lambda_1, \lambda_2, p) \equiv \epsilon_\mu^*(\lambda_1, p) \epsilon_\nu(\lambda_2, p) + \frac{1}{3} \Delta_{\mu\nu}(p) \delta_{\lambda_1\lambda_2}. \quad (18)$$

Using Eq. (15) and the above expression for  $L_{\mu\nu}$ , we obtain

$$\int_0^\infty \frac{dp_0}{2\pi} 2p_0 L_{\mu\nu}(\lambda_1, \lambda_2, p) G_{<}^{\mu\nu}(x, p) = f_{\lambda_1\lambda_2}(x, \mathbf{p}) - \frac{1}{3} \delta_{\lambda_1\lambda_2} \text{Tr}f(x, \mathbf{p}). \quad (19)$$

So the deviation of  $\rho_{\lambda_1\lambda_2}$  from its equilibrium value (without polarization)  $(1/3)\delta_{\lambda_1\lambda_2}$  can be written as

$$\begin{aligned} \delta\rho_{\lambda_1\lambda_2}(x, \mathbf{p}) &\equiv \rho_{\lambda_1\lambda_2}(x, \mathbf{p}) - \frac{1}{3} \delta_{\lambda_1\lambda_2} \\ &= \frac{\int_0^\infty dp_0 p_0 L_{\mu\nu}(\lambda_1, \lambda_2, p) G_{<}^{\mu\nu}(x, p)}{-\int_0^\infty dp_0 p_0 \Delta_{\mu\nu}(p) G_{<}^{\mu\nu}(x, p)}. \end{aligned} \quad (20)$$

Since  $\rho_{00} - 1/3$  and  $\text{Re}\rho_{-1,1}$  are most relevant to the  $\gamma$  correlator in search for the CME signal [62], we will focus on  $\delta\rho_{00}$  and  $\text{Re}\delta\rho_{-1,1}$  in this paper.

In order to calculate  $\rho_{\lambda_1\lambda_2}$  in Eq. (20), we will evaluate the Green's function  $G_{<}^{\mu\nu}(x, p)$  by expanding  $G_{<}^{\mu\nu}(x, p)$  in powers of external sources: the leading order (LO) contribution  $G_{<, \text{LO}}^{\mu\nu}(x, p)$  without space-time derivatives and the next-to-leading order (NLO) contribution  $G_{<, \text{NLO}}^{\mu\nu}(x, p)$  with space-time derivatives as the linear response correction.

#### IV. DYSON-SCHWINGER EQUATION AND SPECTRAL FUNCTION

In this section, we will derive the spectral function for the  $\rho^0$  meson from the Dyson-Schwinger equation for the two-point Green's function at the leading order. The  $\rho\pi\pi$  vertex is taken from the chiral effective Lagrangian.

##### A. Dyson-Schwinger equation on CTP

We start from the Dyson-Schwinger equation on the CTP for vector mesons [44, 78]

$$G^{\mu\nu}(x_1, x_2) = G_{(0)}^{\mu\nu}(x_1, x_2) + \int_C d^4x'_1 d^4x'_2 G_{(0),\rho}^\mu(x_1, x'_1) \Sigma^\rho_\sigma(x'_1, x'_2) G^{\sigma\nu}(x'_2, x_2), \quad (21)$$

where  $\int_C$  denotes the integral on the CTP contour, and  $\Sigma^{\mu\nu}(x_1, x_2)$  is the self-energy. Acting  $G_{(0)}^{-1, \mu\nu}$  on both sides of Eq. (21), we obtain

$$-i [g_\rho^\mu (\partial_{x_1}^2 + m_V^2) - \partial_{x_1}^\mu \partial_\rho^{x_1}] G^{\rho\nu}(x_1, x_2) = g^{\mu\nu} \delta_C^{(4)}(x_1 - x_2) + \int_C d^4 x' \Sigma_\sigma^\mu(x_1, x') G^{\sigma\nu}(x', x_2), \quad (22)$$

where the delta-function is defined on the CTP

$$\delta_C^{(4)}(x_1 - x_2) = \delta^{(3)}(\mathbf{x}_1 - \mathbf{x}_2) \begin{cases} \delta(x_1^0 - x_2^0), & x_1^0, x_2^0 \in t_+ \\ -\delta(x_1^0 - x_2^0), & x_1^0, x_2^0 \in t_- \\ 0, & \text{otherwise} \end{cases} \quad (23)$$

Here  $t_\pm$  denotes the positive (upper sign) and negative (lower sign) time branch respectively. Using Eqs. (6,7), Eq. (22) can be decomposed into the matrix form

$$\begin{aligned} & -i [g_\rho^\mu (\partial_{x_1}^2 + m_V^2) - \partial_{x_1}^\mu \partial_\rho^{x_1}] \begin{pmatrix} 0 & G_{A,C}^{\rho\nu} \\ G_{R,C}^{\rho\nu} & G_{C,C}^{\rho\nu} \end{pmatrix} (x_1, x_2) \\ & = \begin{pmatrix} 0 & 1 \\ 1 & 0 \end{pmatrix} g^{\mu\nu} \delta^{(4)}(x_1 - x_2) \\ & + \int dx' \begin{pmatrix} \Sigma_{C,\rho}^{\mu,A} & 0 \\ \Sigma_{C,\rho}^{\mu,C} & \Sigma_{R,\rho}^{\mu,C} \end{pmatrix} (x_1, x') \begin{pmatrix} 0 & G_{A,C}^{\rho\nu} \\ G_{R,C}^{\rho\nu} & G_{C,C}^{\rho\nu} \end{pmatrix} (x', x_2). \end{aligned} \quad (24)$$

The Dyson-Schwinger equation for the retarded Green's function  $G_R$  is

$$-i [g_\rho^\mu (\partial_{x_1}^2 + m_V^2) - \partial_{x_1}^\mu \partial_\rho^{x_1}] G_R^{\rho\nu}(x_1, x_2) = g^{\mu\nu} \delta^{(4)}(x_1 - x_2) + \int dx' \Sigma_{R,\rho}^\mu(x_1, x') G_R^{\rho\nu}(x', x_2). \quad (25)$$

Adopting the Wigner transformation defined in Eq. (9) and assuming translation invariance for two-point functions which is equivalent to neglecting space-time derivative terms (nonlocal terms), we obtain the equation for  $G_R$  in momentum space

$$i [g_\rho^\mu (p^2 - m_V^2) - p^\mu p_\rho] G_R^{\rho\nu}(p) = g^{\mu\nu} + \Sigma_{R,\rho}^\mu(p) G_R^{\rho\nu}(p), \quad (26)$$

which is the starting point to derive the spectral function for  $\rho^0$ .

## B. Self-energy

The  $\rho\pi$  interaction can be described by the chiral effective Lagrangian [66]

$$\mathcal{L} = -\frac{1}{4} F^{\mu\nu} F_{\mu\nu} + \frac{1}{2} m_\rho^2 A^\mu A_\mu + |D^\mu \phi|^2 - m_\pi^2 |\phi|^2, \quad (27)$$

where  $A^\mu$  and  $\phi$  denote the field of  $\rho^0$  and  $\pi^\pm$  respectively,  $F_{\mu\nu} = \partial_\mu A_\nu - \partial_\nu A_\mu$  is the field strength tensor for  $\rho^0$ , and  $D_\mu = \partial_\mu - ig_V A_\mu$  is the covariant derivative. The interaction part of the Lagrangian is

$$\mathcal{L}_{\text{int}} = ig_V A^\mu (\phi^\dagger \partial_\mu \phi - \phi \partial_\mu \phi^\dagger) + g_V^2 A_\mu A^\mu \phi^\dagger \phi, \quad (28)$$

where the first and second terms give the  $\rho\pi\pi$  and  $\rho\rho\pi\pi$  vertices respectively.

The Feynman diagrams for the self-energy are shown in Fig. (1). The retarded self-energy is

$$\begin{aligned} \Sigma_R^{\mu\nu}(p) & = \Sigma_F^{\mu\nu}(p) - \Sigma_<^{\mu\nu}(p) \\ & = -g_V^2 \int \frac{d^4 k_1}{(2\pi)^4} \int \frac{d^4 k_2}{(2\pi)^4} (2\pi)^4 \delta^{(4)}(p - k_1 + k_2) (k_1^\mu + k_2^\mu) (k_1^\nu + k_2^\nu) S^F(k_1) S^F(k_2) \\ & + g_V^2 \int \frac{d^4 k_1}{(2\pi)^4} \int \frac{d^4 k_2}{(2\pi)^4} (2\pi)^4 \delta^{(4)}(p - k_1 + k_2) (k_1^\mu + k_2^\mu) (k_1^\nu + k_2^\nu) S^<(k_1) S^>(k_2) \\ & + 2g_V^2 ig^{\mu\nu} \int \frac{d^4 k}{(2\pi)^4} \frac{i}{k^2 - m_\pi^2 + i\epsilon} \\ & = I_{\text{vac}}^{\mu\nu}(p) + I_{\text{med}}^{\mu\nu}(p), \end{aligned} \quad (29)$$

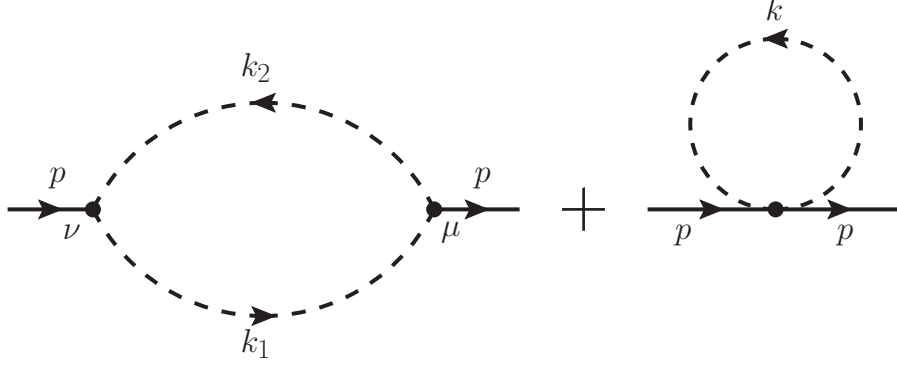


Figure 1: The Feynman diagrams for the self-energy term of  $\rho^0$  meson with momentum  $p$ . The solid line and dashed line denote the propagators of  $\rho^0$  and  $\pi^\pm$  meson respectively, and the arrow on the  $\pi$  propagator denotes the momentum direction of  $\pi^+$ .

where  $I_{\text{vac}}^{\mu\nu}(p)$  and  $I_{\text{med}}^{\mu\nu}(p)$  denote the vacuum and medium parts respectively. They can be put into the forms [66],

$$\begin{aligned} I_{\text{vac}}^{\mu\nu}(p) &= i\Delta^{\mu\nu}(p)\Pi_{\text{vac}}(p), \\ I_{\text{med}}^{\mu\nu}(p) &= i\Delta_L^{\mu\nu}(p)\Pi_{L,\text{med}}(p) + i\Delta_T^{\mu\nu}(p)\Pi_{T,\text{med}}(p), \end{aligned} \quad (30)$$

where the transverse and longitudinal projectors are defined as

$$\begin{aligned} \Delta_L^{\mu\nu}(p) &\equiv \frac{\Delta^{\mu\rho}u_\rho\Delta^{\nu\sigma}u_\sigma}{\Delta^{\rho\sigma}u_\rho u_\sigma}, \\ \Delta_T^{\mu\nu}(p) &\equiv \Delta^{\mu\nu} - \Delta_L^{\mu\nu}. \end{aligned} \quad (31)$$

Here  $u^\mu$  is the flow velocity, in the comoving frame, it becomes  $u^\mu = u_\mu = (1, \mathbf{0})$ . In Eq. (30),  $\Pi_{\text{vac}}$ ,  $\Pi_{L,\text{med}}$  and  $\Pi_{T,\text{med}}$  are given as

$$\Pi_{\text{vac}} = \frac{g_V^2}{(4\pi)^2} p^2 \int_0^1 dx (2x-1)^2 \left[ \log \left| \frac{m_\pi^2 - x(1-x)p^2}{m_\pi^2 - x(1-x)m_\rho^2} \right| - i\pi\theta(x(1-x)p^2 - m_\pi^2) \right], \quad (32)$$

$$\begin{aligned} \Pi_{L,\text{med}}(p) &= \frac{g_V^2}{8\pi^2} \frac{p^2}{|\mathbf{p}|^2} \left[ -4J_0(-1, 2) + \frac{2}{|\mathbf{p}|} (J_+(p, 1, 1) + J_-(p, 1, 1)) \right. \\ &\quad \left. + \frac{2p_0}{|\mathbf{p}|} (J_+(p, 0, 1) - J_-(p, 0, 1)) + \frac{p_0^2}{2|\mathbf{p}|} (J_+(p, -1, 1) + J_-(p, -1, 1)) \right], \end{aligned} \quad (33)$$

$$\begin{aligned} \Pi_{T,\text{med}}(p) &= \frac{g_V^2}{8\pi^2} \left[ \frac{2(p_0^2 + |\mathbf{p}|^2)}{|\mathbf{p}|^2} J_0(-1, 2) + \frac{1}{|\mathbf{p}|} (J_+(p, -1, 3) + J_-(p, -1, 3)) \right. \\ &\quad - \frac{(p^2)^2}{4|\mathbf{p}|^3} (J_+(p, -1, 1) + J_-(p, -1, 1)) - \frac{p^2 p_0}{|\mathbf{p}|^3} (J_+(p, 0, 1) - J_-(p, 0, 1)) \\ &\quad \left. - \frac{p_0^2}{|\mathbf{p}|^3} (J_+(p, 1, 1) + J_-(p, 1, 1)) \right], \end{aligned} \quad (34)$$

where momentum functions  $J_{\pm}(p, n_1, n_2)$  and  $J_0(n_1, n_2)$  are defined as

$$J_+(p, n_1, n_2) \equiv \int_0^\infty d|\mathbf{k}| E_k^{n_1} |\mathbf{k}|^{n_2} [f_{\pi^+}(E_k) + f_{\pi^-}(E_k)] \\ \times \ln \frac{p^2 + 2p_0 E_k + 2|\mathbf{p}||\mathbf{k}| + i\epsilon}{p^2 + 2p_0 E_k - 2|\mathbf{p}||\mathbf{k}| + i\epsilon}, \quad (35)$$

$$J_-(p, n_1, n_2) \equiv \int_0^\infty d|\mathbf{k}| E_k^{n_1} |\mathbf{k}|^{n_2} [f_{\pi^+}(E_k) + f_{\pi^-}(E_k)] \\ \times \ln \frac{p^2 - 2p_0 E_k + 2|\mathbf{p}||\mathbf{k}| + i\epsilon}{p^2 - 2p_0 E_k - 2|\mathbf{p}||\mathbf{k}| + i\epsilon}, \quad (36)$$

$$J_0(n_1, n_2) \equiv \int_0^\infty d|\mathbf{k}| E_k^{n_1} |\mathbf{k}|^{n_2} [f_{\pi^+}(E_k) + f_{\pi^-}(E_k)]. \quad (37)$$

In Eqs. (35-37), We have assumed that  $\pi^\pm$  are in thermal equilibrium, so  $f_{\pi^+}$  and  $f_{\pi^-}$  are Bose-Einstein distribution depending on the temperature  $T$  and chemical potential  $\pm\mu_\pi$ . Here we have written the self-energy in the same forms as in our previous work [52], and one can prove that it is identical to the results in Ref. [66].

Finally, the total self-energy can be written as

$$\Sigma_R^{\mu\nu} = i\Delta_L^{\mu\nu}\Pi_L + i\Delta_T^{\mu\nu}\Pi_T, \quad (38)$$

where  $\Pi_L$  and  $\Pi_T$  are defined as

$$\Pi_L \equiv \Pi_{\text{vac}} + \Pi_{L,\text{med}}, \\ \Pi_T \equiv \Pi_{\text{vac}} + \Pi_{T,\text{med}}. \quad (39)$$

Note that Eqs. (35-37) are results in the flow's comoving frame. To obtain their expressions in the lab frame we have to make a Lorentz boost. In this paper, we work in the flow's comoving frame.

### C. Spectral function

Inserting Eq. (38) into Eq. (26), we can solve  $G_R^{\mu\nu}(p)$  as a function of  $\Pi_L$  and  $\Pi_T$ ,

$$G_R^{\mu\nu}(p) = \frac{-i}{p^2 - m_V^2 - \Pi_L} \Delta_L^{\mu\nu} + \frac{-i}{p^2 - m_V^2 - \Pi_T} \Delta_T^{\mu\nu} + \frac{i}{m_V^2} \frac{p^\mu p^\nu}{p^2}, \quad (40)$$

where we have used

$$\Delta_{L,\rho}^\mu \Delta_L^{\rho\nu} = \Delta_L^{\mu\nu}, \quad \Delta_{T,\rho}^\mu \Delta_T^{\rho\nu} = \Delta_T^{\mu\nu}, \\ \Delta_{L,\rho}^\mu \Delta_T^{\rho\nu} = p_\mu \Delta_L^{\mu\nu} = p_\mu \Delta_T^{\mu\nu} = 0. \quad (41)$$

We can read out the longitudinal and transverse spectral function from Eq. (40) as

$$\rho_L(p) = -\text{Im} \frac{1}{p^2 - m_V^2 - \Pi_L}, \\ \rho_T(p) = -\text{Im} \frac{1}{p^2 - m_V^2 - \Pi_T}. \quad (42)$$

From the relation  $\tilde{G}_{<}^{\mu\nu}(p) = 2in_B(p_0)\text{Im}\tilde{G}_R^{\mu\nu}(p)$  [79, 80] ( $G_i^{\mu\nu} = i\tilde{G}_i^{\mu\nu}$  for  $i = <, >, F, \bar{F}, G, A$ ), the leading order Wigner function reads

$$G_{<,\text{LO}}^{\mu\nu}(p) = -2n_B(p^0) [\Delta_L^{\mu\nu} \rho_L(p) + \Delta_T^{\mu\nu} \rho_T(p)]. \quad (43)$$

Here  $n_B(p_0)$  is the Bose-Einstein distribution. Inserting Eq. (43) into Eq. (20), we can obtain the leading order contribution to the spin density matrix.

## V. LINEAR RESPONSE THEORY

In this section, we will derive the NLO correction to the Wigner function by linear response theory. We will use the Kubo formula derived in Zubarev's approach [63–65].

The linear response of an observable  $\langle \hat{O}(x) \rangle$  for the operator  $\hat{O}(x)$  to the perturbation  $\partial_\mu \beta_\nu$  reads [65]

$$\begin{aligned} \langle \hat{O}(x) \rangle - \langle \hat{O}(x) \rangle_{\text{LE}} &= \partial_\mu \beta_\nu(x) \lim_{K^\mu \rightarrow 0} \frac{\partial}{\partial K_0} \\ &\times \text{Im} \left[ iT(x) \int_{-\infty}^t d^4x' \langle [\hat{O}(x), T^{\mu\nu}(x')] \rangle_{\text{LE}} e^{-iK \cdot (x' - x)} \right], \end{aligned} \quad (44)$$

where  $\langle \hat{O}(x) \rangle \equiv \text{Tr} [\hat{\rho} \hat{O}(x)]$  is the expectation value in non-equilibrium while  $\langle \hat{O}(x) \rangle_{\text{LE}} \equiv \text{Tr} [\hat{\rho}_{\text{LE}} \hat{O}(x)]$  is the expectation value in local equilibrium,  $\hat{\rho}$  and  $\hat{\rho}_{\text{LE}}$  are non-equilibrium and local equilibrium density operators respectively,  $\beta^\mu(x) \equiv u^\mu(x)/T(x)$  with  $u^\mu(x)$  and  $T(x)$  being the flow velocity and temperature respectively, and  $T^{\mu\nu}$  is the energy-momentum tensor for the vector field give by

$$T^{\mu\nu} = F_\rho^\mu F^{\rho\nu} + m_V^2 A^\mu A^\nu - g^{\mu\nu} \left( -\frac{1}{4} F_{\rho\sigma} F^{\rho\sigma} + \frac{1}{2} m_V^2 A_\rho A^\rho \right). \quad (45)$$

We choose the operator  $\hat{O}(x)$  in Eq. (44) to be the Wigner function operator

$$\hat{G}_{<}^{\mu\nu}(x, p) \equiv \int d^4y e^{ip \cdot y} A^\nu \left( x - \frac{1}{2}y \right) A^\mu \left( x + \frac{1}{2}y \right). \quad (46)$$

The correction to  $G_{<}^{\mu\nu}(x, p)$  from the perturbation  $\partial_\mu \beta_\nu$  can be written as

$$G_{<,\text{NLO}}^{\mu\nu}(x, p) = 2T \xi_{\gamma\lambda} \frac{\partial n_B(p_0)}{\partial p_0} I^{\mu\nu\gamma\lambda}(p), \quad (47)$$

where  $\xi_{\gamma\lambda} = \partial_{(\gamma} \beta_{\lambda)}$  denotes the thermal shear stress tensor, and the tensor  $I^{\mu\nu\gamma\lambda}(p)$  is defined as

$$\begin{aligned} I^{\mu\nu\gamma\lambda}(p) &\equiv -[g^{\lambda\gamma}(p^2 - m^2) - 2p^\lambda p^\gamma] (\Delta_L^{\mu\nu} \rho_L^2 + \Delta_T^{\mu\nu} \rho_T^2) \\ &+ 2(p^2 - m^2) (\Delta_L^{\mu\lambda} \rho_L + \Delta_T^{\mu\lambda} \rho_T) (\Delta_L^{\nu\gamma} \rho_L + \Delta_T^{\nu\gamma} \rho_T). \end{aligned} \quad (48)$$

The detailed derivation of  $I^{\mu\nu\gamma\lambda}(p)$  can be found in [51, 52].

Now the total Wigner function is

$$G_{<}^{\mu\nu}(x, p) = G_{<,\text{LO}}^{\mu\nu}(x, p) + G_{<,\text{NLO}}^{\mu\nu}(x, p), \quad (49)$$

where the LO and NLO contributions are given by Eqs. (43) and (47) respectively. Inserting Eq. (49) into Eq. (20), the deviation of the spin density matrix from 1/3 can be expressed as

$$\delta\rho_{\lambda_1\lambda_2}(x, \mathbf{p}) = \frac{\int_0^\infty dp_0 p_0 L_{\mu\nu}(\lambda_1, \lambda_2, p) [G_{<,\text{LO}}^{\mu\nu}(x, p) + G_{<,\text{NLO}}^{\mu\nu}(x, p)]}{-\int_0^\infty dp_0 p_0 \Delta_{\mu\nu}(p) [G_{<,\text{LO}}^{\mu\nu}(x, p) + G_{<,\text{NLO}}^{\mu\nu}(x, p)]}. \quad (50)$$

In order to numerically calculate the spin density matrix that can be compared with experimental data in momentum space, we have to integrate over  $x$  on the freeze-out hypersurface for both numerator and denominator in Eq. (50) as

$$\delta\rho_{\lambda_1\lambda_2}(\mathbf{p}) = \frac{\int_0^\infty dp_0 \int d\Sigma^\mu p_\mu L_{\mu\nu}(\lambda_1, \lambda_2, p) [G_{<,\text{LO}}^{\mu\nu}(x, p) + G_{<,\text{NLO}}^{\mu\nu}(x, p)]}{-\int_0^\infty dp_0 \int d\Sigma^\mu p_\mu \Delta_{\mu\nu}(p) [G_{<,\text{LO}}^{\mu\nu}(x, p) + G_{<,\text{NLO}}^{\mu\nu}(x, p)]}, \quad (51)$$

where  $\Sigma^\mu$  is the freeze-out hypersurface. If the system evolves homogeneously in time,  $\Sigma^0$  is actually the space volume, so  $d\Sigma^0 = d^3x$ . The above formula is the starting point for the numerical calculation in the next section.

## VI. NUMERICAL RESULTS

In this section, we will numerically calculate  $\rho_{00}$  and  $\text{Re}\rho_{-1,1}$  by Eq. (51). The parameters are chosen as  $m_\rho = 770$  MeV,  $m_\pi = 139$  MeV,  $g_V = 6.07$  for the  $\rho\pi\pi$  coupling constant [66],  $T = 150$  MeV for the freeze-out temperature. The rapidity range is set to  $|Y| < 1$ . The freeze-out hypersurface and thermal shear stress tensor are calculated by hydrodynamical model CLVisc at  $\sqrt{s_{NN}} = 11.5, 19.6, 27, 39, 62.4$  and 200 GeV and 20-50% centrality [23, 67, 68]. Here we assume that the thermal shear stress tensor does not change a lot before and after hadronization, so we can apply it to the  $\rho\pi$  system.

### A. Results for $\rho_{00}$

From Eq. (51), the LO contribution to  $\rho_{00}$  involves

$$\begin{aligned} L_{\mu\nu}(0, 0, p)G_{<, \text{LO}}^{\mu\nu}(x, p) &= -2 \left( \frac{p_y^2}{|\mathbf{p}|^2} - \frac{1}{3} \right) n_B(p_0) [\rho_T(p) - \rho_L(p)], \\ -\Delta_{\mu\nu}(p)G_{<, \text{LO}}^{\mu\nu}(x, p) &= 2n_B(p_0) [2\rho_T(p) + \rho_L(p)]. \end{aligned} \quad (52)$$

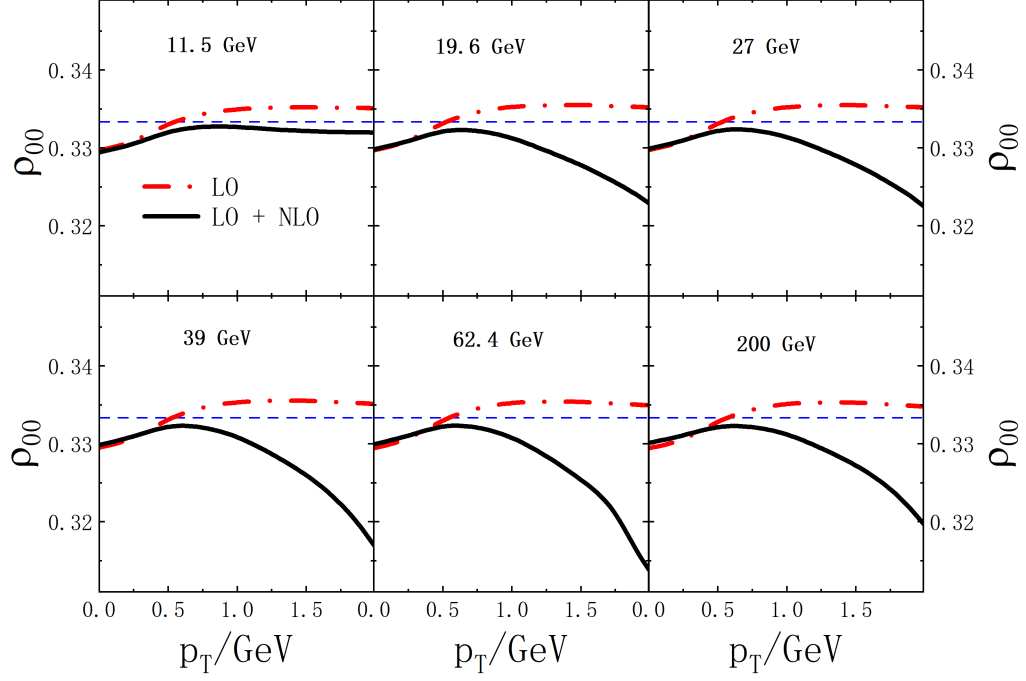
We see that the spin alignment as a function of the momentum may be non-vanishing at the LO although the momentum integrated spin alignment at the same order should be zero. The NLO contribution involves

$$\begin{aligned} L_{\mu\nu}(0, 0, p)G_{<, \text{NLO}}^{\mu\nu}(x, p) &= -2T\xi_{\lambda\gamma} \frac{\partial n_B(p_0)}{\partial p_0} \\ &\times \left\{ [g^{\lambda\gamma} (p^2 - m^2) - 2p^\lambda p^\gamma] L_{\mu\nu}(0, 0, p) (\Delta_L^{\mu\nu} \rho_L^2 + \Delta_T^{\mu\nu} \rho_T^2) \right. \\ &\left. - 2(p^2 - m^2) L_{\mu\nu}(0, 0, p) (\Delta_L^{\mu\lambda} \rho_L + \Delta_T^{\mu\lambda} \rho_T) (\Delta_L^{\nu\gamma} \rho_L + \Delta_T^{\nu\gamma} \rho_T) \right\}, \end{aligned} \quad (53)$$

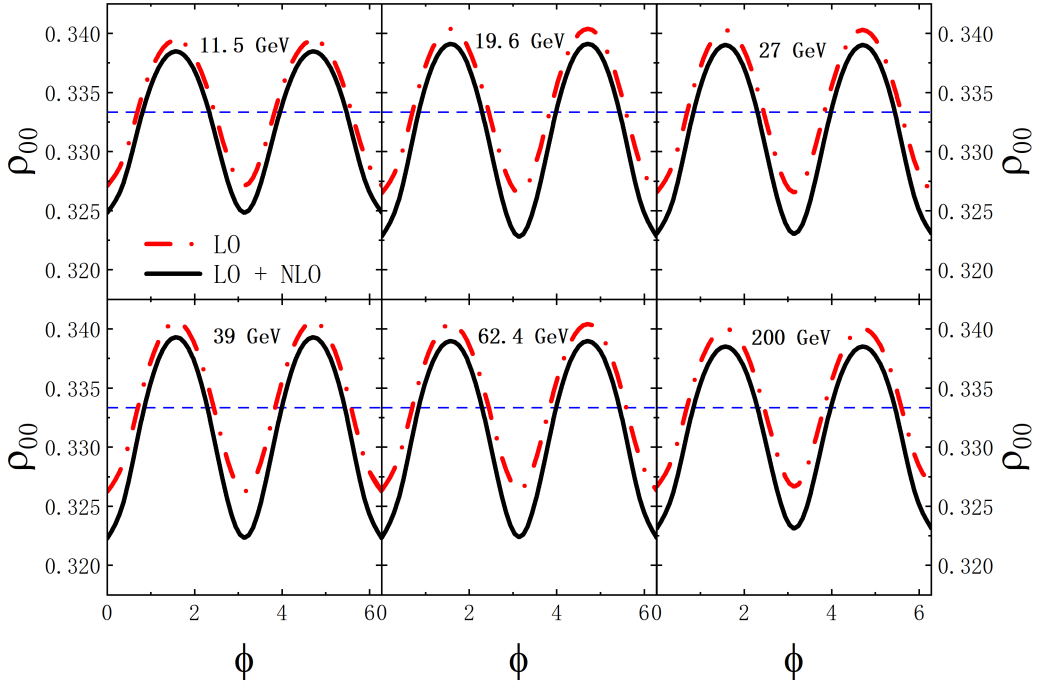
$$\begin{aligned} -\Delta_{\mu\nu}(p)G_{<, \text{NLO}}^{\mu\nu}(x, p) &= 2T\xi_{\lambda\gamma} \frac{\partial n_B(p_0)}{\partial p_0} \left\{ [g^{\lambda\gamma} (p^2 - m^2) - 2p^\lambda p^\gamma] (2\rho_T^2 + \rho_L^2) \right. \\ &\left. - 2(p^2 - m^2) (\Delta_L^{\lambda\gamma} \rho_L^2 + \Delta_T^{\lambda\gamma} \rho_T^2) \right\}. \end{aligned} \quad (54)$$

The NLO contribution is proportional to the thermal shear stress tensor  $\xi_{\lambda\gamma}$ , so it may contribute to the momentum integrated spin alignment. It is important to note that the coefficient of  $\xi_{\lambda\gamma}$  increases with increasing  $p$ , so the expansion will break down for large  $p$ . In other words, the linear response theory only works for low momenta.

The spin alignment as functions of the transverse momentum  $p_T$  and azimuthal angle  $\phi$  in the central rapidity  $|Y| < 1$  is shown in Fig. (2), and  $\rho_{00}$  as functions of the collision energy is shown in Fig. (3). We can see in Fig. (2a) that  $\delta\rho_{00}$  (the spin alignment) at the LO is negative for  $p_T \lesssim 0.5$  GeV and positive for  $p_T \gtrsim 0.5$  GeV but with very small magnitude of the order  $10^{-3}$ , while its NLO contribution is negative and its magnitude increases with  $p_T$  due to the term proportional to  $\xi_{\lambda\gamma} p^\lambda p^\gamma$  in Eqs. (53-54). It turns out that the total values of  $\delta\rho_{00}$  from the LO and NLO are negative in the region up to  $p_T = 2$  GeV. Note that the non-vanishing values of the LO contribution to  $\delta\rho_{00}$  are due to the space-time integration on the freezeout hypersurface and the rapidity range. The azimuthal angle  $\phi$  dependence of  $\delta\rho_{00}$  is shown in Fig. (2b) in an oscillation pattern with the magnitude at the LO being about  $10^{-2}$ . We see that  $\delta\rho_{00}$  is positive for  $\phi = \pi/2, 3\pi/2$  and negative for  $\phi = 0, \pi$ . The NLO contribution to  $\delta\rho_{00}$  is slightly smaller than zero since it is suppressed by  $n_B(p_0)$  for high  $p_T$  in  $p_T$  integration. Fig. (3) shows that the LO contribution to  $\delta\rho_{00}$  is independent of the collision energy, while the NLO contribution is negative and decreases with the collision energy when it is lower than about 50 GeV.



(a)



(b)

Figure 2: The spin alignment of  $\rho^0$  mesons at different collision energies as functions of (a) transverse momentum  $p_T$  and (b) azimuthal angle  $\phi$  in the central rapidity region  $|Y| < 1$ . The red dash-dotted lines are the LO contribution, while the black solid lines are the sum over the LO and NLO contribution.

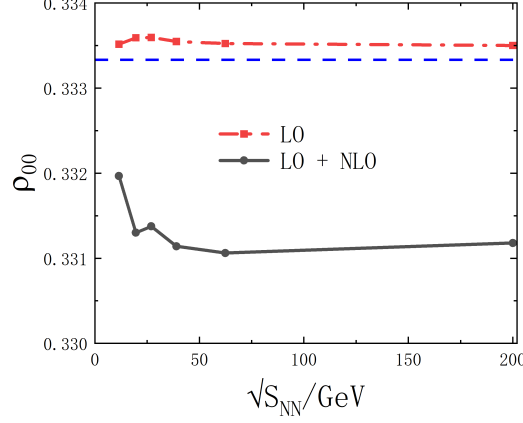


Figure 3: The spin alignment of  $\rho^0$  mesons in the central rapidity region  $|Y| < 1$  as functions of the collision energy.

### B. Results for $\text{Re}\rho_{-1,1}$

From Eq. (51), the LO and NLO contributions to  $\text{Re}\rho_{-1,1}$  involve

$$\begin{aligned} \text{Re}L_{\mu\nu}(-1, 1, p)G_{<, \text{LO}}^{\mu\nu}(x, p) &= -n_B(p_0) \frac{p_x^2 - p_z^2}{|\mathbf{p}|^2} [\rho_T(p) - \rho_L(p)], \\ \text{Re}L_{\mu\nu}(-1, 1, p)G_{<, \text{NLO}}^{\mu\nu}(x, p) &= -2T\xi_{\lambda\gamma} \frac{\partial n_B(p_0)}{\partial p_0} \left\{ [g^{\lambda\gamma} (p^2 - m^2) - 2p^\lambda p^\gamma] \right. \\ &\quad \times \text{Re}L_{\mu\nu}(-1, 1, p) (\Delta_L^{\mu\nu} \rho_L^2 + \Delta_T^{\mu\nu} \rho_T^2) \\ &\quad - 2(p^2 - m^2) \text{Re}L_{\mu\nu}(-1, 1, p) \\ &\quad \left. \times (\Delta_L^{\mu\lambda} \rho_L + \Delta_T^{\mu\lambda} \rho_T) (\Delta_L^{\nu\gamma} \rho_L + \Delta_T^{\nu\gamma} \rho_T) \right\}, \end{aligned} \quad (55)$$

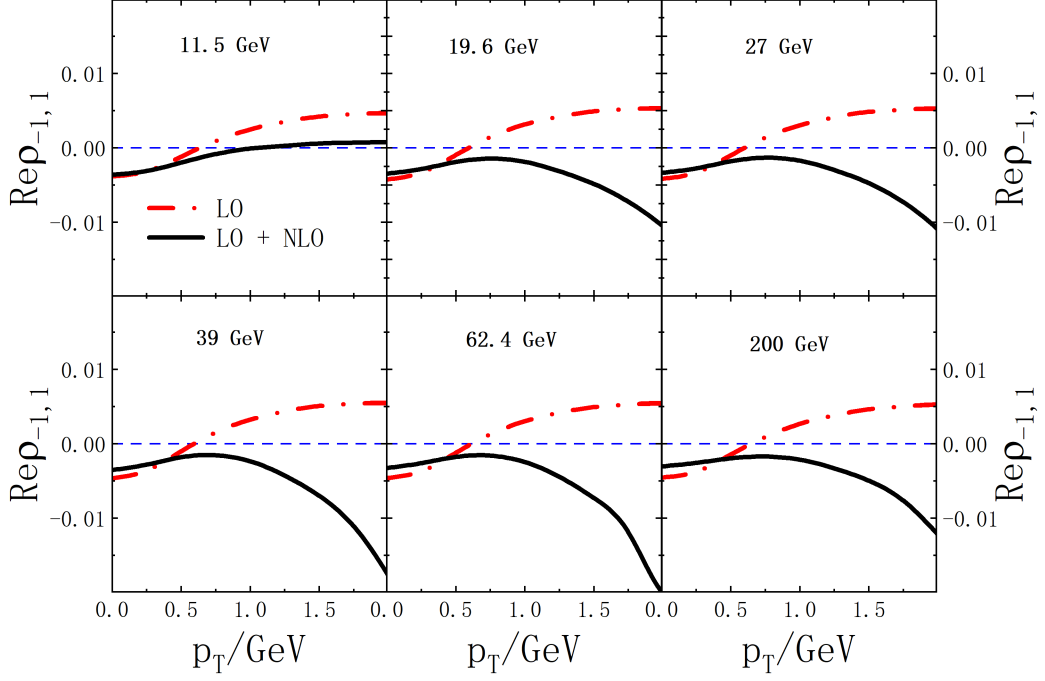
Here the denominator is the same as in  $\rho_{00}$ . Similarly, the LO contribution to  $\text{Re}\rho_{-1,1}$  as a momentum function may be non-vanishing although the momentum integrated one should be vanishing. The NLO contribution may give rise to both integrated and un-integrated non-zero  $\text{Re}\rho_{-1,1}$ .

The off-diagonal element  $\text{Re}\rho_{-1,1}$  as functions of  $p_T$  and  $\phi$  in the central rapidity range  $|Y| < 1$  is presented in Fig. (4), and its dependence on the collision energy is presented in Fig. (5). In Fig. (4a), we can see that the LO contribution is negative for low  $p_T$  and positive for high  $p_T$  with the magnitude of the order  $10^{-3}$ . The NLO contribution is negative and its magnitude increases with  $p_T$ , which is also a result of the  $\xi_{\lambda\gamma} p^\lambda p^\gamma$  term. As shown in Fig. (4b),  $\text{Re}\rho_{-1,1}$  as functions of  $\phi$  has an oscillation pattern similar to  $\delta\rho_{00}$  but with an opposite sign, due to the different signs of  $p_x^2$  terms in Eqs. (52) and (55) (we can express  $p_y^2$  as  $|\mathbf{p}|^2 - p_x^2 - p_z^2$ ). The collision energy dependence of  $\text{Re}\rho_{-1,1}$  also has the similar behavior to  $\delta\rho_{00}$ , as shown in Fig. (5).

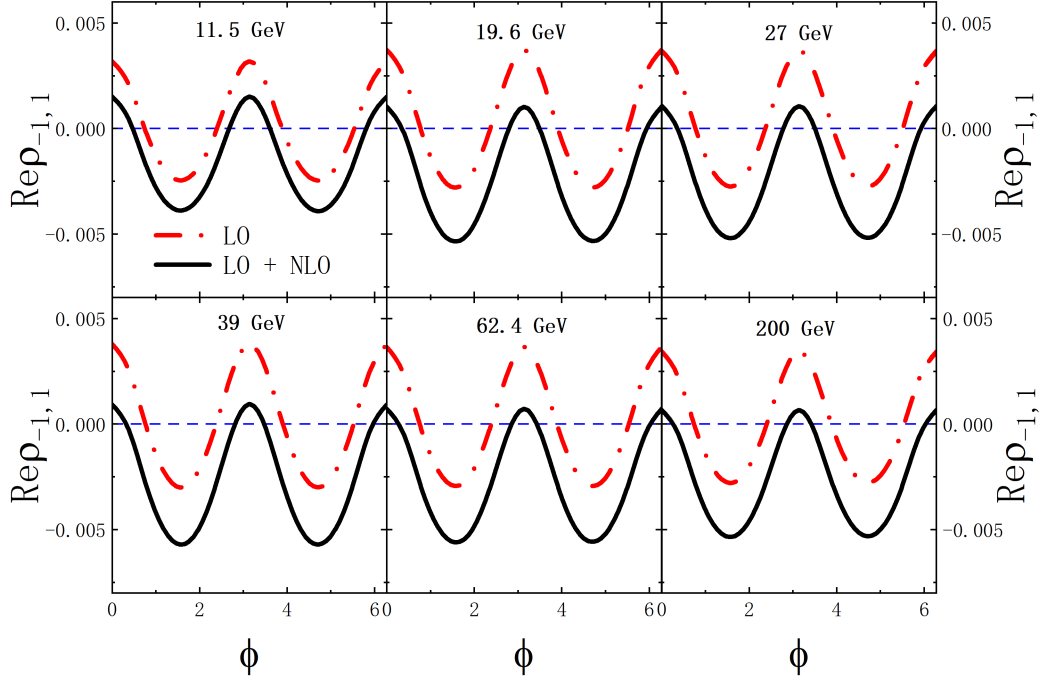
In conclusion, the contributions from the spectral function and from the thermal shear stress tensor to the spin density matrix of  $\rho^0$  mesons are of the order of  $10^{-3} \sim 10^{-2}$ . For un-integrated quantities,  $\delta\rho_{00}(p_T)$  and  $\text{Re}\rho_{-1,1}(p_T)$  are all negative and decrease with  $p_T$ , and  $\delta\rho_{00}(\phi)$  and  $\text{Re}\rho_{-1,1}(\phi)$  show oscillation patterns but with opposite signs. The momentum integrated  $\delta\rho_{00}$  and  $\text{Re}\rho_{-1,1}$  are all negative and decrease with the collision energy when the collision energy is less than about 50 GeV, while they are almost constant when the collision energy is higher.

## VII. SUMMARY AND CONCLUSIONS

We study the spin density matrix of neutral  $\rho$  mesons contributed from the spectral function and thermal shear tensor with the Kubo formula in the linear response theory. We introduce the two-point Green's function in the CTP formalism which defines the Wigner function and the MVSD in phase space for neutral  $\rho$  mesons. As the leading order contribution, the spectral function of the neutral  $\rho$  meson can be obtained from the Dyson-Schwinger equation for the retarded Green's function with  $\rho\pi\pi$  and  $\rho\rho\pi\pi$  interactions in a thermal pion gas. Then the next-to-leading order contribution from the thermal shear tensor can be calculated through the Kubo formula in the linear response



(a)



(b)

Figure 4: The off-diagonal element  $\text{Re}\rho_{-1,1}$  of  $\rho^0$  mesons at different collision energies as functions of (a) transverse momentum  $p_T$  and (b) azimuthal angle  $\phi$  in the central rapidity region  $|Y| < 1$ . The red dash-dotted lines are the LO contribution, while the black solid lines are the sum over the LO and NLO contribution.

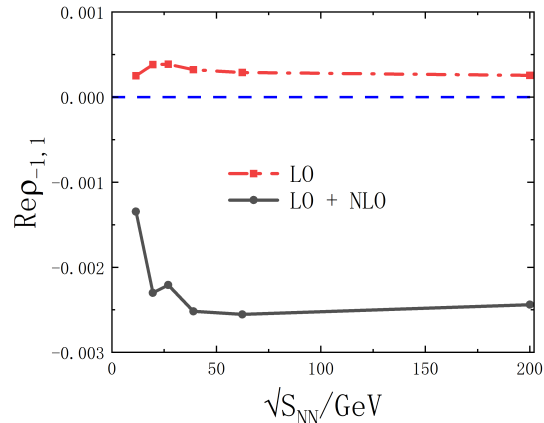


Figure 5: The off-diagonal element  $\text{Re}\rho_{-1,1}$  of  $\rho^0$  mesons in the central rapidity region  $|Y| < 1$  as functions of the collision energy.

theory. Finally we present numerical results for  $\rho_{00}$  and  $\text{Re}\rho_{-1,1}$  which have a dominant effect on the  $\gamma$  correlator in search for the CME. The numerical results for the thermal shear tensor are needed for evaluating the spin density matrix, which can be calculated by hydrodynamical models. The numerical results give negative values for  $\delta\rho_{00}$  and  $\text{Re}\rho_{-1,1}$  as functions of the transverse momentum at the order  $10^{-2}$ , while their values as functions of the azimuthal angle show oscillation patterns. The momentum integrated  $\delta\rho_{00}$  and  $\text{Re}\rho_{-1,1}$  are all negative and decrease with the collision energy when the collision energy is less than about 50 GeV, while they are almost constant for higher collision energies.

#### ACKNOWLEDGMENTS

The work is supported in part by the National Natural Science Foundation of China (NSFC) under Grant No. 12135011.

- 
- [1] S. Barnett, Rev. Mod. Phys. **7**, 129 (1935).
  - [2] A. Einstein and W. de Haas, Deutsche Physikalische Gesellschaft, Verhandlungen **17**, 152 (1915).
  - [3] Z.-T. Liang and X.-N. Wang, Phys. Rev. Lett. **94**, 102301 (2005), nucl-th/0410079, [Erratum: Phys.Rev.Lett. 96, 039901 (2006)].
  - [4] S. A. Voloshin, (2004), nucl-th/0410089.
  - [5] Z.-T. Liang and X.-N. Wang, Phys. Lett. B **629**, 20 (2005), nucl-th/0411101.
  - [6] B. Betz, M. Gyulassy, and G. Torrieri, Phys. Rev. C **76**, 044901 (2007), 0708.0035.
  - [7] J.-H. Gao *et al.*, Phys. Rev. C **77**, 044902 (2008), 0710.2943.
  - [8] F. Becattini, F. Piccinini, and J. Rizzo, Phys. Rev. C **77**, 024906 (2008), 0711.1253.
  - [9] STAR, L. Adamczyk *et al.*, Nature **548**, 62 (2017), 1701.06657.
  - [10] STAR, J. Adam *et al.*, Phys. Rev. C **98**, 014910 (2018), 1805.04400.
  - [11] HADES, R. Abou Yassine *et al.*, Phys. Lett. B **835**, 137506 (2022), 2207.05160.
  - [12] ALICE, S. Acharya *et al.*, Phys. Rev. Lett. **128**, 172005 (2022), 2107.11183.
  - [13] I. Karpenko and F. Becattini, Eur. Phys. J. C **77**, 213 (2017), 1610.04717.
  - [14] H. Li, L.-G. Pang, Q. Wang, and X.-L. Xia, Phys. Rev. C **96**, 054908 (2017), 1704.01507.
  - [15] Y. Xie, D. Wang, and L. P. Csernai, Phys. Rev. C **95**, 031901 (2017), 1703.03770.
  - [16] Y. Sun and C. M. Ko, Phys. Rev. C **96**, 024906 (2017), 1706.09467.
  - [17] M. Baznat, K. Gudima, A. Sorin, and O. Teryaev, Phys. Rev. C **97**, 041902 (2018), 1701.00923.
  - [18] S. Shi, K. Li, and J. Liao, Phys. Lett. B **788**, 409 (2019), 1712.00878.
  - [19] D.-X. Wei, W.-T. Deng, and X.-G. Huang, Phys. Rev. C **99**, 014905 (2019), 1810.00151.
  - [20] B. Fu, K. Xu, X.-G. Huang, and H. Song, Phys. Rev. C **103**, 024903 (2021), 2011.03740.
  - [21] S. Ryu, V. Jupic, and C. Shen, Phys. Rev. C **104**, 054908 (2021), 2106.08125.
  - [22] X.-G. Deng, X.-G. Huang, and Y.-G. Ma, (2021), 2109.09956.

- [23] X.-Y. Wu, C. Yi, G.-Y. Qin, and S. Pu, *Phys. Rev. C* **105**, 064909 (2022), 2204.02218.
- [24] Q. Wang, *Nucl. Phys.* **A967**, 225 (2017), 1704.04022.
- [25] W. Florkowski, A. Kumar, and R. Ryblewski, *Prog. Part. Nucl. Phys.* **108**, 103709 (2019), 1811.04409.
- [26] X.-G. Huang, J. Liao, Q. Wang, and X.-L. Xia, (2020), 2010.08937.
- [27] J.-H. Gao, Z.-T. Liang, Q. Wang, and X.-N. Wang, *Lect. Notes Phys.* **987**, 195 (2021), 2009.04803.
- [28] J.-H. Gao, G.-L. Ma, S. Pu, and Q. Wang, *Nucl. Sci. Tech.* **31**, 90 (2020), 2005.10432.
- [29] Y.-C. Liu and X.-G. Huang, *Nucl. Sci. Tech.* **31**, 56 (2020), 2003.12482.
- [30] F. Becattini, *Rept. Prog. Phys.* **85**, 122301 (2022), 2204.01144.
- [31] Y. Hidaka, S. Pu, Q. Wang, and D.-L. Yang, *Prog. Part. Nucl. Phys.* **127**, 103989 (2022), 2201.07644.
- [32] F. Becattini *et al.*, *Int. J. Mod. Phys. E* **33**, 2430006 (2024), 2402.04540.
- [33] G. Bunce *et al.*, *Phys. Rev. Lett.* **36**, 1113 (1976).
- [34] K. Schilling, P. Seyboth, and G. E. Wolf, *Nucl. Phys. B* **15**, 397 (1970), [Erratum: *Nucl.Phys.B* 18, 332 (1970)].
- [35] Y.-G. Yang, R.-H. Fang, Q. Wang, and X.-N. Wang, *Phys. Rev. C* **97**, 034917 (2018), 1711.06008.
- [36] A. H. Tang *et al.*, *Phys. Rev. C* **98**, 044907 (2018), 1803.05777, [Erratum: *Phys.Rev.C* 107, 039901 (2023)].
- [37] STAR, M. S. Abdallah *et al.*, *Nature* **614**, 244 (2023), 2204.02302.
- [38] X.-L. Xia, H. Li, X.-G. Huang, and H. Zhong Huang, *Phys. Lett. B* **817**, 136325 (2021), 2010.01474.
- [39] J.-H. Gao, *Phys. Rev. D* **104**, 076016 (2021), 2105.08293.
- [40] B. Müller and D.-L. Yang, *Phys. Rev. D* **105**, L011901 (2022), 2110.15630.
- [41] A. Kumar, B. Müller, and D.-L. Yang, *Phys. Rev. D* **108**, 016020 (2023), 2304.04181.
- [42] X.-L. Sheng, L. Oliva, and Q. Wang, *Phys. Rev. D* **101**, 096005 (2020), 1910.13684, [Erratum: *Phys.Rev.D* 105, 099903 (2022)].
- [43] X.-L. Sheng, Q. Wang, and X.-N. Wang, *Phys. Rev. D* **102**, 056013 (2020), 2007.05106.
- [44] X.-L. Sheng, L. Oliva, Z.-T. Liang, Q. Wang, and X.-N. Wang, (2022), 2206.05868.
- [45] X.-L. Sheng, L. Oliva, Z.-T. Liang, Q. Wang, and X.-N. Wang, *Phys. Rev. Lett.* **131**, 042304 (2023), 2205.15689.
- [46] X.-L. Sheng, S. Pu, and Q. Wang, *Phys. Rev. C* **108**, 054902 (2023), 2308.14038.
- [47] J. Chen, Z.-T. Liang, Y.-G. Ma, and Q. Wang, *Sci. Bull.* **68**, 874 (2023), 2305.09114.
- [48] X.-L. Sheng, Z.-T. Liang, and Q. Wang, *Acta Phys. Sin.* (in Chinese) **72**, 072502 (2023).
- [49] J. Chen *et al.*, *Nucl. Phys. News* **34**, 17 (2024).
- [50] J.-H. Chen, Z.-T. Liang, Y.-G. Ma, X.-L. Sheng, and Q. Wang, *Sci. China Phys. Mech. Astron.* **68**, 211001 (2025), 2407.06480.
- [51] F. Li and S. Y. F. Liu, (2022), 2206.11890.
- [52] W.-B. Dong, X.-L. Sheng, Y.-L. Yin, and Q. Wang, Global polarization and spin alignment in heavy-ion collisions: past, present and future, in *25th International Spin Symposium*, 2024, 2401.15576.
- [53] D. Kharzeev, *Phys. Lett. B* **633**, 260 (2006), hep-ph/0406125.
- [54] D. E. Kharzeev, L. D. McLerran, and H. J. Warringa, *Nucl. Phys. A* **803**, 227 (2008), 0711.0950.
- [55] K. Fukushima, D. E. Kharzeev, and H. J. Warringa, *Phys. Rev. D* **78**, 074033 (2008), 0808.3382.
- [56] S. A. Voloshin, *Phys. Rev. C* **70**, 057901 (2004), hep-ph/0406311.
- [57] STAR, L. Adamczyk *et al.*, *Phys. Rev. C* **88**, 064911 (2013), 1302.3802.
- [58] STAR, L. Adamczyk *et al.*, *Phys. Rev. C* **89**, 044908 (2014), 1303.0901.
- [59] F. Wang and J. Zhao, *Phys. Rev. C* **95**, 051901 (2017), 1608.06610.
- [60] A. H. Tang, *Chin. Phys. C* **44**, 054101 (2020), 1903.04622.
- [61] D. Shen, J. Chen, A. Tang, and G. Wang, *Phys. Lett. B* **839**, 137777 (2023), 2212.03056.
- [62] Y.-L. Yin, W.-B. Dong, J.-Y. Pang, S. Pu, and Q. Wang, (2024), 2402.03672.
- [63] D. N. Zubarev, A. V. Prozorkevich, and S. A. Smolyanskii, *Theoretical and Mathematical Physics* **40**, 821 (1979).
- [64] A. Hosoya, M.-a. Sakagami, and M. Takao, *Annals Phys.* **154**, 229 (1984).
- [65] F. Becattini, M. Buzzegoli, and E. Grossi, *Particles* **2**, 197 (2019), 1902.01089.
- [66] C. Gale and J. I. Kapusta, *Nucl. Phys. B* **357**, 65 (1991).
- [67] L.-G. Pang, H. Petersen, and X.-N. Wang, *Phys. Rev. C* **97**, 064918 (2018), 1802.04449.
- [68] X.-Y. Wu, G.-Y. Qin, L.-G. Pang, and X.-N. Wang, *Phys. Rev. C* **105**, 034909 (2022), 2107.04949.
- [69] P. C. Martin and J. S. Schwinger, *Phys. Rev.* **115**, 1342 (1959).
- [70] L. V. Keldysh, *Zh. Eksp. Teor. Fiz.* **47**, 1515 (1964).
- [71] K.-c. Chou, Z.-b. Su, B.-l. Hao, and L. Yu, *Phys. Rept.* **118**, 1 (1985).
- [72] J.-P. Blaizot and E. Iancu, *Phys. Rept.* **359**, 355 (2002), hep-ph/0101103.
- [73] Q. Wang, K. Redlich, H. Stoecker, and W. Greiner, *Phys. Rev. Lett.* **88**, 132303 (2002), nucl-th/0111040.
- [74] J. Berges, *AIP Conf. Proc.* **739**, 3 (2004), hep-ph/0409233.
- [75] W. Cassing, *Eur. Phys. J. ST* **168**, 3 (2009), 0808.0715.
- [76] M. Crossley, P. Glorioso, and H. Liu, *JHEP* **09**, 095 (2017), 1511.03646.
- [77] W.-B. Dong, Y.-L. Yin, X.-L. Sheng, S.-Z. Yang, and Q. Wang, *Phys. Rev. D* **109**, 056025 (2024), 2311.18400.
- [78] D. Wagner, N. Weickgenannt, and E. Speranza, (2023), 2306.05936.
- [79] A. Fetter and J. Walecka, *Quantum Theory of Many-particle Systems* Dover Books on Physics (Dover Publications, 2003).
- [80] D. Zubarev, V. Morozov, and G. Röpke, *Statistical Mechanics of Nonequilibrium Processes, Statistical Mechanics of Nonequilibrium Processes. Volume 2: Relaxation and Hydrodynamic Processes* Statistical Mechanics of Nonequilibrium Processes (Wiley, 1997).